CO_2 laser surface patterning of nylon 6,6 and the subsequent effects on wettability characteristics and apatite response.

D.G. Waugh and J. Lawrence

School of Engineering, University of Lincoln, Lincoln, Lincolnshire, LN6 7TS, UK

1.0 – Abstract.

Simulated body fluid (SBF) has been used previously to predict the osseointegration potential of materials by assesing the apatite response. This paper details a study carried out using a CO_2 laser to induce a number of surface patterns which inherently modified both the surface chemistry and surface topography of nylon 6,6 and gave rise to a difference in apatite response. These induced patterns caused a reduction in hydrophilicity with increased contact angles of up to 10°. Following immersion in SBF for 14 days each sample was weighed revealing an increase in weight of up to 0.029 g indicating that an apatite layer had begun to form. Energy dispersive X-ray (EDX) analysis identified the presence of calcium and phosphorous, two elements which support osteoblast cell response. It was found that the laser induced patterned samples gave rise to more layer crystals forming suggesting a more optimized surface for osteoblast cell growth.

Keywords: CO_2 laser, nylon 6,6, wettability, biocompatibility, simulated body fluid (SBF).

2.0 – Introduction

It has been demonstrated previously that polymers can be used for biological applications [1,2]. With respect to the biomaterial, various materials such as metals, ceramics and polymers have been used for biomedical implants [3-6]. Nylon is a low cost family of semi-crystalline engineering thermoplastics with the most common being that of nylon 6 and nylon 6,6. Owed to the material properties nylon 6,6 possesses it can be seen that this polymer has been used for such biological applications as sutures [3], vascular grafts [4] and other hard tissue implants [7] . What is more, by modifying the surface of polymeric materials it may be

possible to identify other biological applications as this may enhance the biomimetic and biocompatible properties. The polymer surface can be optimised for these various applications through surface modification where either the surface topography or surface chemistry is altered. These modifications can be brought about by using numerous methods such as radiation grafting [8], lithography [9], coating technologies [10] and plasma surface modification [11].

Laser surface patterning [2,5] offers a convenient means of modifying the surface of a material on both the micro- and nano-scale without compromising the bulk properties of the material, which can be seen to be of great importance when applied to fields such as biomimetics. This is on account of previous work which has identified a high dependence of the modifications on cell-material interactions [6]. Laser surface treatment offers numerous advantages such as it can be accurate, precise and non-contact allowing one to see that this can be a relatively clean process. In addition, with small heat affect zones (HAZ) lasers allow one to have the ability to modify both the surface chemistry and topography simultaneously without changing the bulk properties which may already be sufficient for the intended application. Furthermore, lasers also offer the opportunity of inducing varying levels of topography depending on how the laser is employed. For instance, periodic patterns can be induced using a focused beam whereas a more random pattern can be employed using a larger, more divergent, laser beam.

One can deduce from the literature that a change in the surface chemistry or surface topography will greatly affect the wettability characteristics of a material [12]. As a direct result of this, it would be a great advantage to those throughout the biomedical industry if, by knowing the wettability of a material, one could predict how a material will react in the

intended application. This would lead to scientific, economic and clinical benefits. For instance, by enhancing bio-implants and having the ability to estimate the biofunctionality of these devices, ultimately this will reduce the need for unnecessary post-implantation surgery, will reduce the amount of discomfort and pain patients will be in and will give rise to a reduction in the failure rate.

Simulated body Fluid (SBF) has been used in the past by others to aid in predicting the bioactivity and osseointegration potential of materials [13]. This is owed to the fact that the bioactivity of almost all orthopaedic biomaterials has a strong relationship with the ability of that material to promote the formation of bone-like carbonate apatite crystals [1,13,14]. What is more, this apatite crystal layer associates specific bone proteins which are crucial for any form of bone reconstruction to commence [15]. Under healthy normal conditions, body fluid is known to usually be already supersaturated with respect to apatite and, upon nucleation of the apatite, the layer can grow through the consumption of the calcium and phosphate ions present in the body fluid. It should also be noted here that employing SBF experiments *in vitro* does not fully reproduce the *in vivo* environment for bone formation, as stated by Roach et al. [6] these *in vitro* techniques involving SBF allow for a sufficient rapid screening of materials in the endeavour of development and optimization.

On account of the potential of laser surface treatment for polymeric biomaterials, this paper details the effects of soaking nylon 6,6 samples in SBF after CO_2 laser patterning. In addition to this, the characteristic wettability for each sample studied was determined in the endeavour to link wettability to the resulting response of the samples being immersed in SBF.

3.0 – Experimental Techniques

3.1 – CO_2 laser patterning procedure, topography, wettability and surface chemistry

The details of how the CO_2 laser patterning procedure and analysis of topography, wettability and surface chemistry have been detailed before by Waugh *et al* [2]. Five samples were used for this experimentation; As-received (AR), 50 μm trench (T50), 50 μm hatch (H50), 100 μm trench (T100) and 100 μm hatch (H100) patterns.

3.2 – *In vitro* simulated body fluid (SBF) experimentation

Simulated body fluid (SBF) is a liquid which has inorganic ion concentrations equivalent to those of human extracellular fluid (human blood plasma). The SBF was prepared by using a magnetic stirrer hotplate (RCT Basic; IKA, GmbH) keeping the solution at a constant temperature of 36.5°C. 500 ml of distilled water was put into an autoclaved 1000 ml beaker and stirred until the constant temperature of 36.5°C was reached. At this time the chemicals given in Table 1 were added in order until the sodium sulphate (#9) had been added.

Once the sodium sulphate (#9 in Table 1) had been added the Tris(hydroxymethyl) aminomethane (#10 in Table 1) was supplemented into the solution less than a gram at a time in order to avoid local increase of pH. Finally, in order to adjust the pH value to 7.4 hydrogen chloride (#11 in Table 1) was added and the beaker was then filled to 1000 ml using distilled water. The samples were then placed into sterile 30 ml glass containers, immersed in 30 ml of SBF and placed into an incubator to keep the temperature constant at 37°C for seven days.

3.3 – SEM, EDX and optical microscopy analysis of immersed samples

Prior to being immersed in the SBF the nylon 6,6 samples were weighed using a balance (S-403; Denver Instrument, GmbH) with a readability of 0.001g. Once the 14 days had elapsed the samples were removed from the SBF, rinsed lightly with distilled water and allowed to air dry in a clean room. Once fully dry the samples were weighed and the difference in weight before and after being immersed in the SBF was determined. Following this the samples were gold coated and analysed using optical microscopy and scanning electron microscopy (SEM). Furthermore, the samples were analysed using EDX in order to identify elements present after the immersion in SBF.

4 – Results and Discussion

4.1 – Effects of CO_2 laser patterning on topography

From Figure 1 it can be seen that the CO_2 laser patterning gave rise to significant modification of the nylon 6,6 surfaces in terms of topography. That is, the laser patterned samples (see Figures 1(b) – (e)) appeared to qualitatively have a considerably larger roughness in comparison to the 3-D profile of the as-received sample (see Figure 1(a)). It was deduced that the CO_2 laser-induced patterned samples had considerably rougher surfaces with the largest peak heights being of the order of 2 μm (see Figure 1(b) to Figure 1(e)) in contrast to the as-received sample (see Figure 1(a)) which had peaks heights of up to 0.2 μm. On account of the increase in peak heights over the CO_2 laser-patterned samples the surface roughness (see Table 2) increased considerably with the largest Sa of 0.4 μm being achieved with the 50 μm hatch sample (CH50) and largest Ra of 0.2 μm for the 100 μm trench sample (CT100). It is given in Table 2 that the patterned samples with scan dimensions of 50 μm

(samples CT50 and CH50) had larger Sa roughness values when compared to the samples patterned with 100 μm scan dimensions (samples CT100 and CH100). This can be attributed to the fact that the 50 μm scan dimensions irradiated more of the sample giving rise to an increase of mass being melted and re-solidified. Also, it can be seen from the Table 2 that the roughness for the hatch patterns had decreased in comparison to the trench patterns. This can be explained by the laser re-melting sections of the nylon 6,6 surface owed to the scanning process of the system. By re-melting these sections the material could then have re-solified into a smoother surface topography.

4.2 – Effects of CO_2 laser patterning on wettability characteristics

From previous work [2] and available literature [16] it can be seen that surface properties, which are reported to have major influences on the wettability characteristics [17], have the potential to be modified using numerous techniques. Table 2 shows that the roughness had considerably increased using the laser patterning (samples T50, T100 – H100) in comparison to the as-received sample (AR). This contrast can be identified through the Sa and Ra roughness parameters insofar as the as-received sample (AR) had an Sa and Ra of 0.126 and 0.029 μm, respectively, where the Sa and Ra for the laser patterned samples increased by up to 0.51 and 0.156 μm, respectively.

The polar component, γ^P, and total surface energy, γ^T, two parameters known to potentially affect the wettability [5], decreased significantly for the laser patterned samples (T50, T100 – H100). This reduction in surface energies, along with increased surface roughness brought about an apparent increase in contact angle inherently making the nylon 6,6 less hydrophilic. These observations do not necessarily coincide with current theory [5] which states that for a

significant increase in surface roughness a hydrophilic material ought to produce a more hydrophilic surface with the contact angle effectively decreasing [18]. It is possible to explain this phenomena by the plausible existence of a mixed state wetting regime, in which both Wenzel and Cassie-Baxter regimes are present over the solid-liquid interface [19].

Hao and Lawrence [5] found that a rise in surface oxygen content in turn gave rise to a reduction in the contact angle. But Table 2 suggests the resulting surface oxygen content in this work may not be the main contributing factor in determining the outcome of the contact angle. This is due to the modified wettability characteristics not having an apparent correlative trend with the rise in surface oxygen content observed.

Finally, the results obtained as seen in Table 2 attests an evident and significant rise in contact angle which can be attributed to the reduction in apparent surface energies, γ^P and γ^T, which arise as a direct result of the mixed state wetting regime can be ascribed to the liquid-surface interaction owed to variations in the laser-induced surface topography. As in previous work [2], it can then be extrapolated that both the closely linked apparent surface energies and surface topography appear to be the main driving force in the resulting contact angle.

4.3 – Effects of CO_2 laser patterning on simulated body fluid (SBF) response

From Figure 2 it was observed that only a very small amount of sediment was present on the as-received sample (see Figure 2(a)) in comparison to the other samples which had undergone CO_2 laser-induced patterning (see Figures 2(b) to (e)). This was also confirmed by weighing the samples before and after the immersion in SBF as can be seen in Figure 3. That is, the laser patterned samples weighed at least 0.008 g more than compared to the as-

received sample. It is also apparent from Figure 2(b) and Figure 2(e) that the sediment preferentially forms around craters formed due to evolved gases breaking at the surface during the melting taking place following the CO_2 laser processing. This highlights that it may be possible to construct a polymeric surface which allows selective apatite formation giving rise to selective positioning for the growth of osteoblast cells.

From the contact angle results given in Table 2 and the difference in mass shown in Figure 3 it is possible to ascertain that an increase in contact angle has appeared to have a more positive impact on apatite response. What is more, this enhancement in the promotion of apatite layers forming could also be attributed to the significant increase in surface roughness.

Through EDX analysis (see Figure 4) it was found that following the formation of the apatite crystals, phosphorous and calcium was present on the surface of the nylon 6,6 samples. This is of importance due to phosphorous and calcium having to be present in order for an apatite to form which would inherently increase the bioactivity of the material. The sediments analysed also incorporated sodium, magnesium and chlorine which had all been present in the SBF and indicates that these elements would also make up some of the apatite layer formed.

5.0 – Conclusions

It has been shown through experimentation that a relatively inexpensive CO_2 laser marker has the ability to significantly modify the surface properties of nylon 6,6. For instance, the characteristic contact angle increased for the laser patterned samples increased by up to 10° in comparison to the as-received sample. This can be explained by the likelyhood of a mixed-state wetting regime which arises through the patterning of the material surface. What is

more, the surface modifications have also been seen to have a positive impact on the formation of apatite layers under immersion in simulated body fluid (SBF), implying that enhanced osteoblast cell response can be achieved using CO_2 laser surface treatment when compared to the as-received sample. This research has identified that this is likely to have a major impact upon the biomaterials industry in terms of economic and clinical factors. That is, the laser-induced enhanced apatite response has highlighted that it is likely failure rates can be decreased, patient comfort increased and the need for post-implantation surgery being dramatically reduced.

6.0 – Acknowledgements

The authors would like to thank their collaborators: Directed Light Inc., East Midlands NHS Innovation Hub, Nobel Biocare and Photomachining Inc. for all of their much appreciated support. The authors greatly acknowledge Chemical Engineering, Loughborough University for use of their biological laboratory. This study is also financially supported by the EPSRC (EP/E046851/1).

7.0 – References

1. M. Nagano, T. Kitsugi, T. Nakamura, T. Kokubo and M. Tanahashi, J. Biomed. Mater. Res., 1996, 31, 487-494.

2. D.G.Waugh, J. Lawrence, D.J. Morgan and C.L.Thomas, Mater. Sci. Eng. C, 2009, 29, 2514-2524.

3. C. Mao, W. Zhao, C. Zhu, A. Zhu, J. Shen and S. Lin, Carbohyd. Polym., 2005, 59, 19-25.

4. E. Karaca and A.S. Hockenberger, J. Biomed. Mater. Res. B: Appl. Biomat., 2008, 87, 580-589.

5. L. Hao and J. Lawrence, 'Laser surface treatment of bio-implant materials', 2005, New Jersey, USA: John Wiley & Sons Inc.

6. P. Roach, D. Eglin, K. Rohde and C.C. Perry, J. Mater. Sci.: Mater. Med., 2007, 18, 1263-1277.

7. M. Makropoulou, A.A. Serafetinides and C.D. Skordoulis, Lasers Med. Sci., 1995, 10, 201-206.

8. R.S. Benson, Nucl. Inst. Meth. Phys. Res. B, 2002, 191, 752-757.

9. C. David, J. Wei, T. Lippert and A. Wokaun, Microelec. Eng., 2001, 57-58, 453-460.

10. Q. Zhao, C. Wang, Y. Liu and S. Wang, Int. J. Adh. Adh., 2007, 27, 85-91.

11. P.K. Chu, Surf. Coat. Technol., 2007, 201, 8076-8082.

12. Y.C. Jung and B. Bhushan, Scripta Materialia, 2007, 57, 1057-1060.

13. W.H. Song, Y.K. Jun, Y. Han and S.H. Han, Biomaterials, 2004, 25, 3341-3349.

14. L. Hao, J. Lawrence and L. Li, Appl. Surf. Sci., 2005, 247, 453-457.

15. C. Rey, J. Biomech., 1998, 31, 182-182.

16. S. Dadbin, Euro. Polym. J., 2002, 38, 2489-2495.

17. J. Zhang, J. Kang, P. Hu and Q. Meng, Appl. Surf. Sci., 2007, 253, 5436-5441.

18. Y.C. Jung and B. Bhushan, Nanotechnol., 2006, 17, 4970-4980.

19. S.M. Lee and T.H. Kwon, J. Micromech. Microeng. 2007, 17, 687-692.

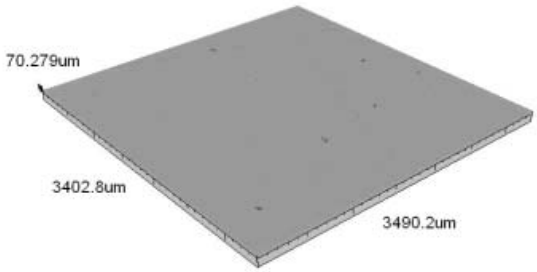

(a)

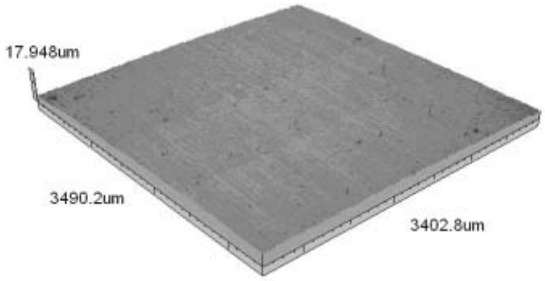

(b)

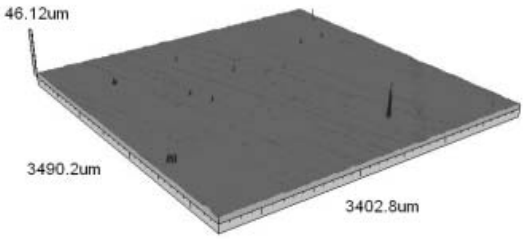

(c)

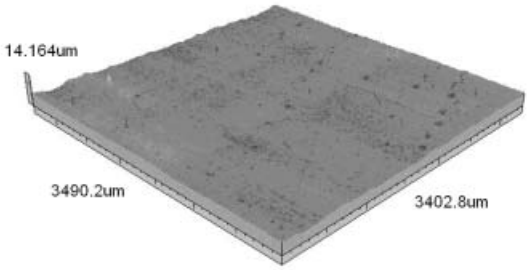

(d)

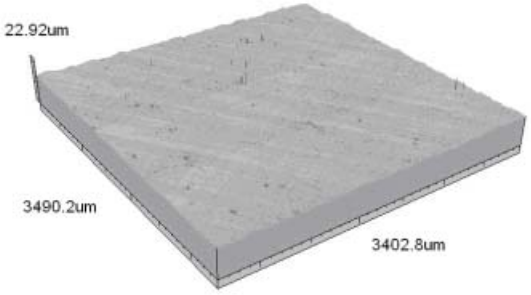

(e)

Figure 1 – Continuous axonometric images for each of the nylon 6,6 samples – (a) As-received (AR) (b) 50 µm trench (T50) (c) 100 µm (T100) (d) 50 µ hatch (H50) and (e) 100 µm hatch (H100).

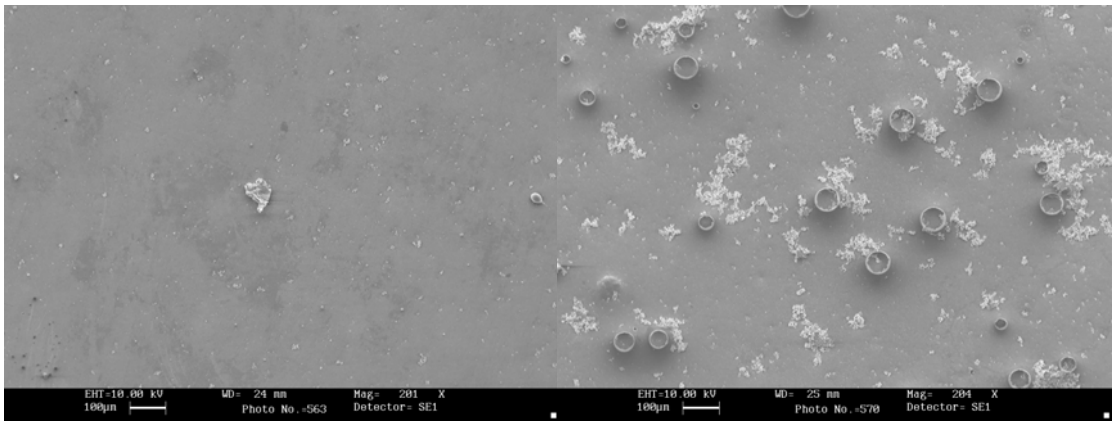

(a) (b)

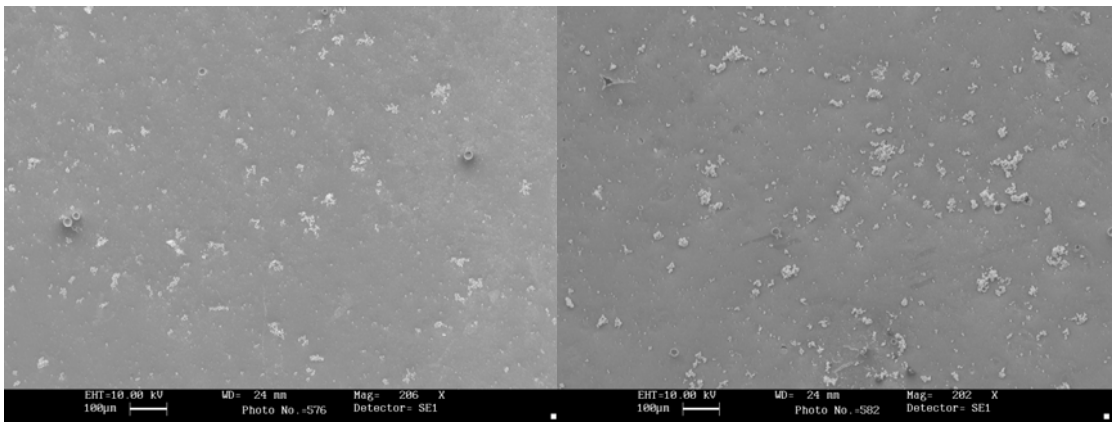

(c) (d)

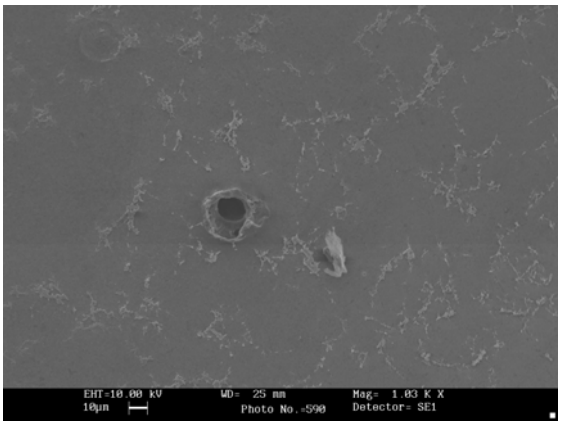

(e)

Figure 2 – SEM images of (a) AR, (b) T50, (c) T100, (d) H50 and (e) H100 after immersion in SBF for 14 days.

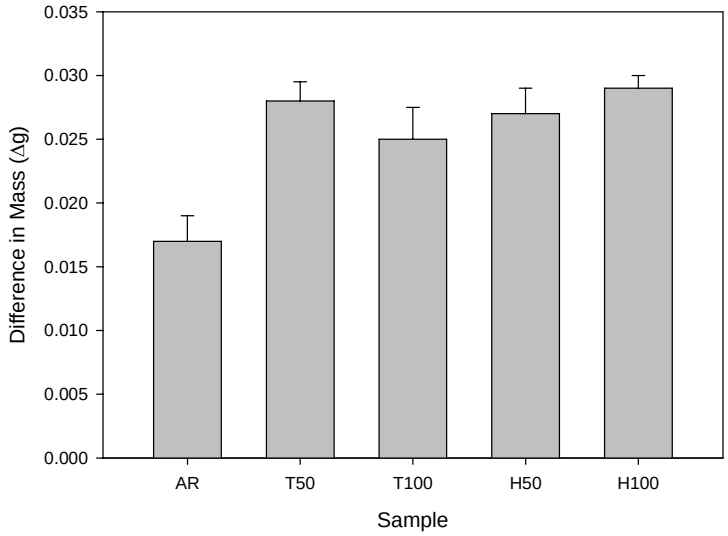

Figure 3 – Difference in mass before and after immersion in SBF for all samples.

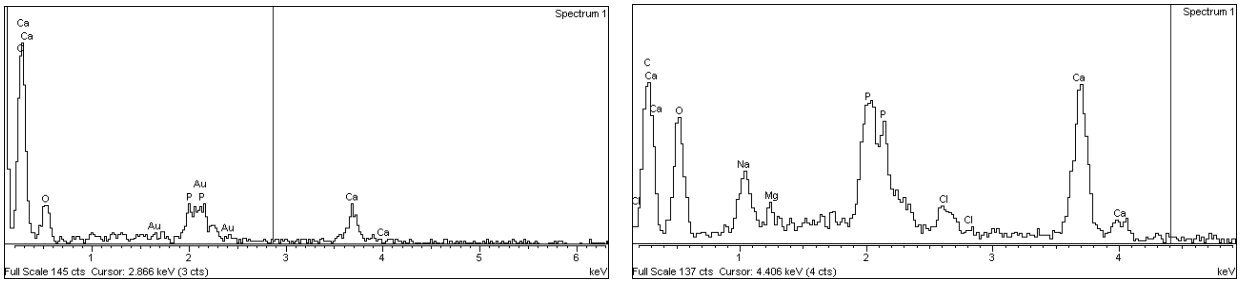

(a) (b)

Figure 4 - EDX spectra of (a) the as-received sample (AR) and (b) a typical CO_2 laser surface modified sample following immersion in SBF after 14 days.

Table 1 – Amounts and order of reagents to prepare 1000 ml SBF

Order	Reagent	Amount
1	Distilled water	750 ml
2	(NaCl)	7.996 g
3	($NaHCO_3$)	0.350 g
4	(KCl)	0.224 g
5	($K_2HPO_4 \cdot 3H_20$)	0.228 g
6	($MgCl_2 \cdot 6H_20$)	0.305 g
7	(~0.1 M in H_2O) (HCl)	40 ml
8	($CaCl_2$)	0.278 g
9	(Na_2SO_4)	0.071 g
10	$(CH_2OH)_3CNH_2$	6.057 g
11	(~0.1 M in H_2O) (HCl)	Adj. of pH

Table 2 – Measured values for surface roughness, contact angle and surface energy parameters for each sample.

Sample ID	**Sa** (μm)	**Ra** (μm)	γ^P (mJm^{-2})	γ^D (mJm^{-2})	γ^T (mJm^{-2})	**Surface Oxygen Content** (%at.)	**Contact Angle** (°)
AR	0.126	0.029	17.69	29.66	47.34	13.26	56.4±1.2
T50	0.636	0.148	12.24	28.63	40.87	14.33	66.0±4.0
T100	0.297	0.185	16.86	29.83	46.69	14.05	57.5±2.4
H50	0.423	0.103	10.93	31.64	42.58	14.99	65.8±2.9
H100	0.326	0.155	13.63	30.37	44.00	14.84	62.2±2.3